LETTERS
PUBLISHED ONLINE: 23 JANUARY 2017 | DOI: 10.1038/NCLIMATE3203
nature climate change

Macroclimatic change expected to transform coastal wetland ecosystems this century

Christopher A. Gabler[1,2*], Michael J. Osland[3], James B. Grace[3], Camille L. Stagg[3], Richard H. Day[3], Stephen B. Hartley[3], Nicholas M. Enwright[3], Andrew S. From[3], Meagan L. McCoy[4] and Jennie L. McLeod[5]

Coastal wetlands, existing at the interface between land and sea, are highly vulnerable to climate change[1–3]. Macroclimate (for example, temperature and precipitation regimes) greatly influences coastal wetland ecosystem structure and function[4,5]. However, research on climate change impacts in coastal wetlands has concentrated primarily on sea-level rise and largely ignored macroclimatic drivers, despite their power to transform plant community structure[6–12] and modify ecosystem goods and services[5,13]. Here, we model wetland plant community structure based on macroclimate using field data collected across broad temperature and precipitation gradients along the northern Gulf of Mexico coast. Our analyses quantify strongly nonlinear temperature thresholds regulating the potential for marsh-to-mangrove conversion. We also identify precipitation thresholds for dominance by various functional groups, including succulent plants and unvegetated mudflats. Macroclimate-driven shifts in foundation plant species abundance will have large effects on certain ecosystem goods and services[5,14–16]. Based on current and projected climatic conditions, we project that transformative ecological changes are probable throughout the region this century, even under conservative climate scenarios. Coastal wetland ecosystems are functionally similar worldwide, so changes in this region are indicative of potential future changes in climatically similar regions globally.

The global extent of coastal wetlands has decreased in recent decades[17] despite their exceptional ecological and economic value[18,19]. The vulnerability of coastal wetlands to sea-level rise is considered so severe that concurrent changes in macroclimate (for example, temperature and precipitation regimes) are often overlooked[5]. Relatively speaking, the effects of macroclimatic change on coastal wetland plant community structure remain largely unexplored[2,5], even though macroclimate is central to climate change studies in terrestrial systems[20] and known to govern foundation plant species distributions in coastal wetlands worldwide[5]. This gap is important because foundation plant species provide many ecosystem services underlying coastal wetlands' exceptional value (for example, storm protection, nutrient removal, carbon sequestration, and fish and wildlife habitat)[6,18,19]. Shifts in foundation species abundance can have considerable ecological and economic effects[6,12–14].

In coastal wetlands around the world, macroclimatic conditions govern which general habitat types are present[5] (Fig. 1): mangrove forests in warm, wet zones[21]; graminoid-dominated marshes in cool, wet zones[22]; succulent-dominated marshes in more arid zones; and unvegetated flats in extremely arid/saline zones[23]. Generally, mangroves outcompete graminoids for light but are sensitive to freezing[2,9,24–26], so sigmoidal relationships between extreme winter air temperatures and mangrove prevalence are observed[6,7]. Similarly, total vegetation abundance has a sigmoidal relationship with precipitation, and coverage decreases as drought/salinity stress intensifies[11,12,27]. These sigmoidal relationships indicate the existence of threshold temperature and precipitation values for the replacement of foundation plant species, and the potential for rapid ecological change in areas near climatic thresholds. Salt marshes and mangroves are both highly valued ecosystems, but the ecological implications of mangrove expansion remain unclear[5–7]. Likewise, succulent and unvegetated wetlands are highly valued[11]; however, the ecosystem goods and services provided by these habitat types differ considerably[5,12]. For example, differences among these habitats in vegetation height and standing biomass are readily apparent, and this has implications for their primary productivity, wildlife habitat value, carbon storage, and storm protection[5,6,12–19].

Due to data constraints, previous studies of macroclimatic controls in coastal wetlands have relied on landscape-scale remotely sensed data available at coarse resolutions. Therefore, those analyses could not quantify detailed changes in functional groups or vegetation structure across climatic gradients[5]. Here, we utilize extensive field data, collected across temperature and precipitation gradients along the northern Gulf of Mexico (NGOM) coast, to develop macroclimatic models that predict dominance by individual functional groups and vegetation structure. Based upon prior studies and ecological descriptions in the literature, we hypothesized strong nonlinear relationships between macroclimatic drivers (that is, minimum air temperature and mean annual precipitation) and the abundance and structure of plant functional groups (that is, mangrove, graminoid, succulent, and unvegetated). Further, based upon current macroclimatic conditions and climate projections for the next century in the NGOM, we also hypothesized that macroclimatic change will transform many NGOM coastal wetland ecosystems.

To quantify and test hypothesized relationships between macroclimate and coastal wetland plant community structure, we collected data from ten estuaries across targeted temperature and precipitation gradients along the NGOM coast (Supplementary Table 1 and Methods). Within each estuary, we defined tidal saline

[1]Department of Biology and Biochemistry, University of Houston, Houston, Texas 77204, USA. [2]School of Earth, Environmental, and Marine Sciences, The University of Texas Rio Grande Valley, Brownsville, Texas 78520, USA. [3]US Geological Survey, Wetland and Aquatic Research Center, Lafayette, Louisiana 70506, USA. [4]McCoy Consulting, Lafayette, Louisiana 70506, USA. [5]McLeod Consulting, Lafayette, Louisiana 70506, USA.
*e-mail: christopher.gabler@utrgv.edu

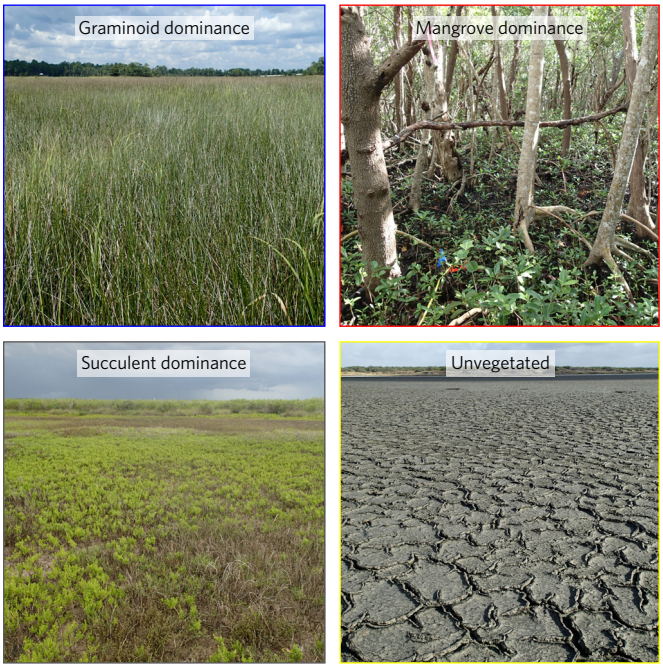

Figure 1 | Four plant functional groups dominate tidal saline wetlands across the northern Gulf of Mexico coast. Photographs by C. A. Gabler.

wetland zone boundaries based on plant communities (Supplementary Table 2) and calculated mean boundary elevations (Supplementary Table 3), which let us standardize and subdivide our data in each estuary. In total, we observed 39 plant species within the tidal saline wetland zone (Supplementary Table 4). Four functional groups—graminoids, mangroves, succulents, and unvegetated flats—dominated the tidal saline wetland zone. Functional group dominance within each estuary's tidal saline wetland zone was greatly influenced by macroclimatic drivers (Figs 2 and 3).

To quantify observed relationships between macroclimate and plant communities, we fit a series of nonlinear least squares (NLS) regression models (Supplementary Table 5) relating dominance of each functional group to minimum surface air temperature (minT) and mean annual precipitation (MAP) observed from 1981–2010 (Methods). As expected, there was a negative sigmoidal relationship between minT and graminoid dominance and a positive sigmoidal relationship between minT and mangrove dominance (Fig. 3a). These sigmoidal relationships demonstrate, as hypothesized[6,7], that there is a temperature threshold for mangrove dominance in the region; in certain coastal reaches, small changes in temperature can trigger large changes in graminoid and/or mangrove dominance[6,7]. We identified positive sigmoidal relationships between MAP and both the proportion of vegetated plots and the total vegetation cover. Cover decreased rapidly where MAP was between ~500 and 1,000 mm yr^{-1} (Fig. 3b). The strong relationship between precipitation and vegetation abundance confirms our hypothesis and validates image-based analyses[11,12]. Individual functional groups followed different rainfall-driven patterns. We identified: a positive sigmoidal relationship between MAP and graminoid plus mangrove dominance; a normal (Gaussian) relationship between MAP and succulents (which peaked under relatively dry conditions at 975 mm yr^{-1}); and a negative sigmoidal relationship between MAP and unvegetated flats (which reflects total vegetation patterns) (Fig. 3b). Marsh-to-mangrove and vegetated-to-unvegetated transitions are expected to affect certain ecosystem services (for example, storm protection, nutrient capture/cycling, carbon storage), erosion, responses to sea-level rise, and fish and wildlife habitat[5,6,11,12,15].

To quantify relationships between macroclimate and vegetation structure, we fit NLS regression models relating minT or MAP to vegetation height, photosynthetically active radiation (PAR) interception, and a biomass proxy (Supplementary Table 5 and Methods). These relationships are discussed in Supplementary Appendix 1. Generally, height and biomass had positive sigmoidal relationships with minT (Fig. 3c) and MAP (Fig. 3d), but the greatest variability was associated with minT and reflected marsh–mangrove transitions.

Because temperature and precipitation can vary independently, we combined our nonlinear equations to create bivariate macroclimatic models for each plant functional group (Supplementary Table 5). We used these bivariate models to calculate predicted dominance for each group across relevant climatic ranges based on minT and MAP. We employed heat maps and contour plots to illustrate the distribution of each functional group across macroclimatic gradients (Fig. 4).

To evaluate the potential effects of macroclimatic change on plant community structure in NGOM tidal saline wetlands, we identified the ranges of minT and MAP observed within six coastal reaches of the NGOM from 1981–2010 (Methods). Then, we developed climate envelope rectangles to illustrate modelled functional group dominance within these six coastal reaches (Fig. 5a, left; Supplementary Fig. 1a, left). The predicted functional group composition within each regional rectangle agrees strongly with observations (Supplementary Table 2 and references therein). We also developed envelopes for vegetation height (Fig. 5a, right; Supplementary Fig. 1a, right) and the biomass proxy (Supplementary Fig. 2a). To illustrate the effects of climate change, we evaluated the ecological change expected under six alternative and realistic climate change scenarios (Methods). We plotted projected climate envelope rectangles for each region and climate scenario onto our maps of functional group dominance (Fig. 5b–d, left; Supplementary Fig. 1b–d, left), vegetation height (Fig. 5b–d, right; Supplementary Fig. 1b–d, right), and the biomass proxy (Supplementary Fig. 2b–g). By comparing current climate envelopes to projected envelopes, one can visualize and quantify potential estuary-scale impacts of climate change on tidal saline wetland plant community structure across the NGOM coast.

As hypothesized, our macroclimatic models show that transformative changes in tidal saline wetland plant community structure are probable across large portions of the NGOM this century. The greatest projected changes in vegetation composition are in Texas, Louisiana, and parts of northern Florida, near the marsh-to-mangrove transition zone (Fig. 5b–d, left; Supplementary Fig. 1b–d, left). Large portions of these coastal reaches are likely to transition from marsh-to-mangrove dominance by 2100[6]. Given the abundance and functional importance of graminoid-dominated wetlands within the region, the ecological implications of woody plant encroachment into these tidal saline wetlands warrants further consideration. Many of the potential impacts on storm protection, nutrient cycling, carbon storage, sediment elevation change, and fish and wildlife habitat are important but unclear.

Changes in precipitation may modulate the effects of warming for some functional groups. For example, increased MAP may lead to mangrove and/or graminoid expansion at the expense of succulent and/or unvegetated wetlands. Conversely, decreased MAP may lead to increases in succulent and/or unvegetated wetlands at the expense of mangrove and/or graminoid-dominated wetlands. The effects of altered MAP will be strongest along coasts with limited rainfall. In freshwater-limited south Texas, drier conditions should result in the expansion of unvegetated salt flats, while wetter conditions should decrease unvegetated dominance. The impacts of these transitions on wildlife utilization, primary production, storm protection, nutrient absorption, and carbon storage merit further

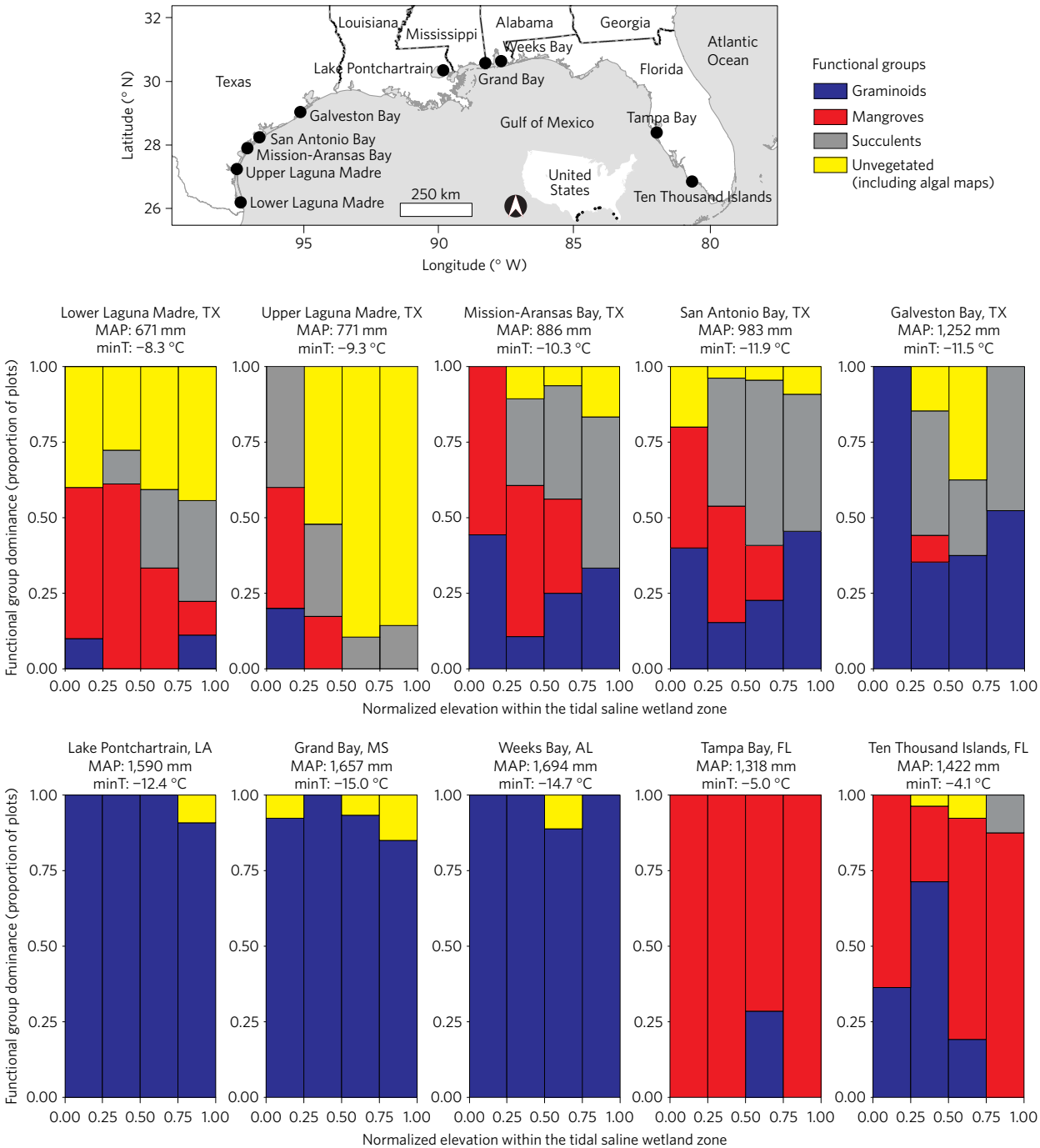

Figure 2 | Distribution of tidal saline wetland plant functional groups across elevation gradients in ten estuaries spanning the northern Gulf of Mexico. The map shows the locations of ten focal estuaries. Stacked bars denote estuary-scale dominance of functional groups within elevation quartiles in the tidal saline wetlands of focal estuaries. MAP, mean annual precipitation (mm yr^{-1}); minT, minimum surface air temperature. Climate values are from 1981–2010 (Methods).

consideration. Projections regarding vegetation height and biomass proxy are discussed in Supplementary Appendix 1.

Since vegetation-dependent ecogeomorphic positive feedbacks greatly influence the ability of coastal wetlands to keep pace with sea-level rise (SLR)[28–30], our results regarding climate-induced vegetation change have important ramifications for models of ecological responses to SLR. SLR is the aspect of climate change expected to have the largest effect upon coastal wetlands. However, scientists and resource managers rarely consider other aspects of climate change, and our aim here was to illustrate the importance of considering macroclimatic drivers and some of the ways that macroclimate shapes coastal wetlands. In response to SLR, coastal wetlands are expected to migrate vertically and horizontally across the landscape. Our analyses do not explicitly incorporate SLR, nor make predictions regarding the landscape positions of tidal saline wetland zones; however, since our models and assumptions reflect the tidal saline wetland zone, these analyses remain relevant under SLR. Our emphasis on macroclimate should not be interpreted as rationale for discounting the importance of SLR. Just as prior SLR studies have not included macroclimatic impacts on coastal wetlands, our current investigation did not include impacts of SLR. In the near future, we anticipate that improved data quality

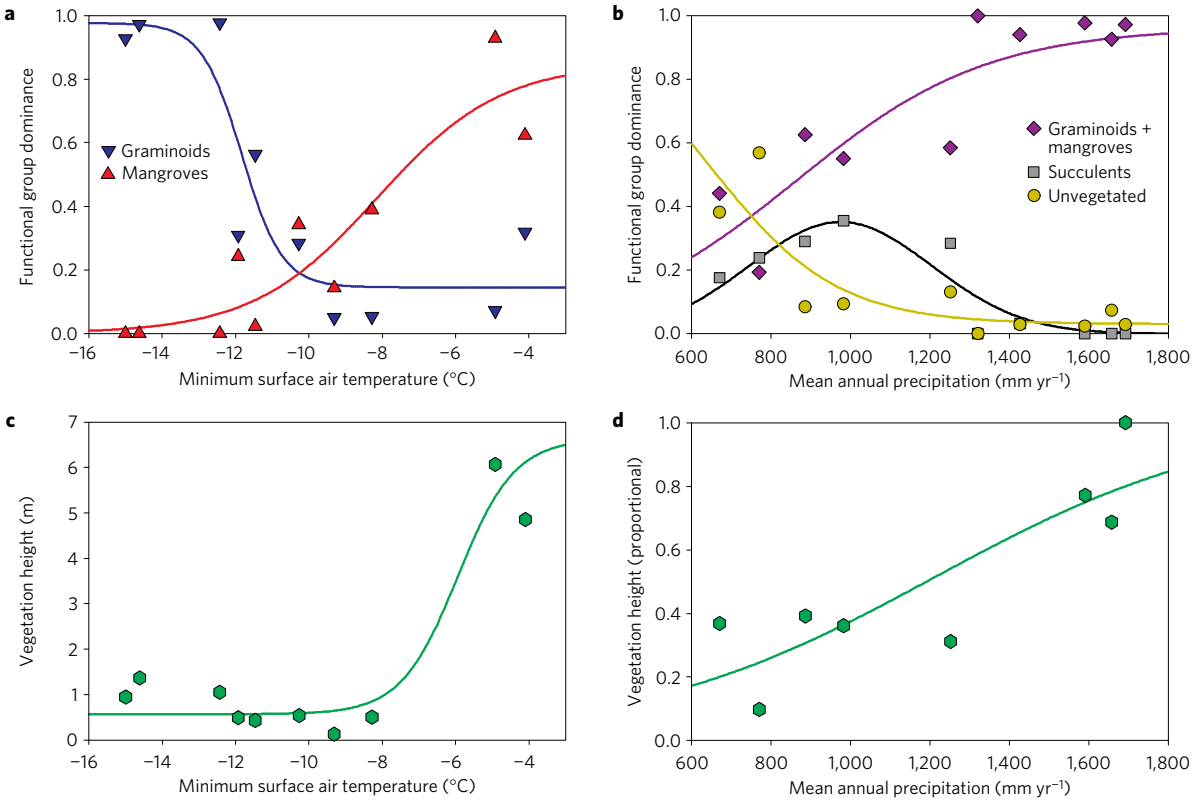

Figure 3 | Nonlinear relationships between macroclimate and tidal saline wetland plant community structure. a, Relationships between minimum surface air temperature and graminoid and mangrove dominance. **b**, Relationships between mean annual precipitation and the dominance of graminoids plus mangroves, succulents and unvegetated. **c**,**d**, Relationships between vegetation height and minimum surface air temperature and mean annual precipitation, respectively. Each point represents one estuary.

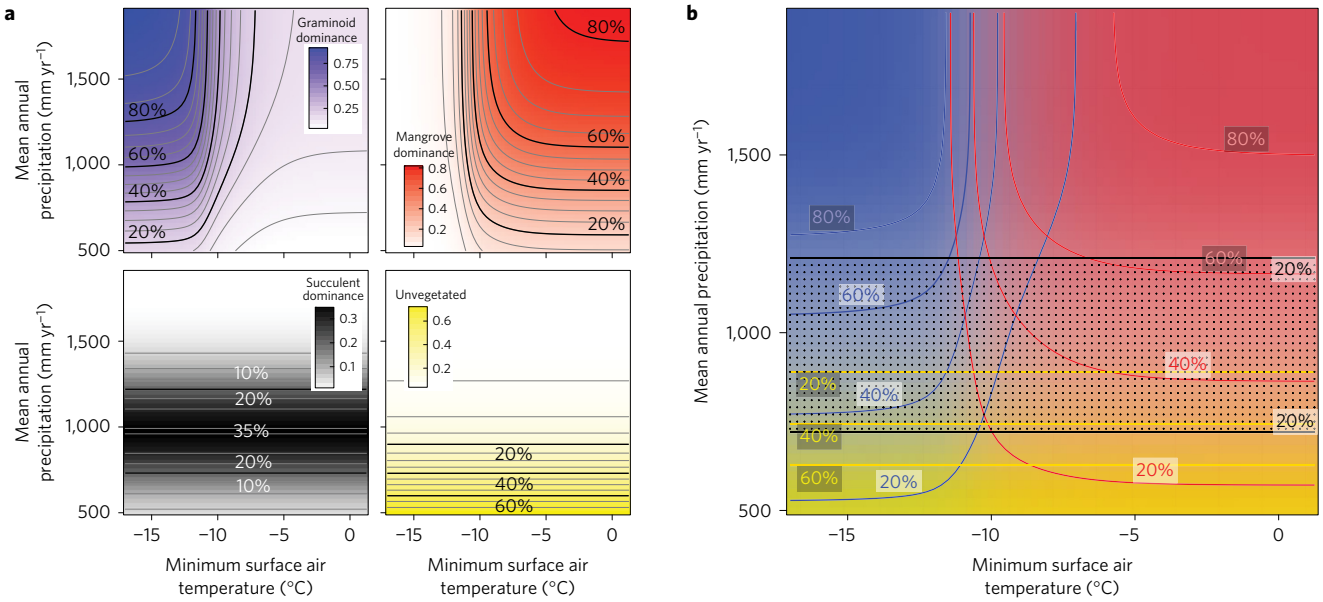

Figure 4 | Distributions of the dominant plant functional groups in northern Gulf of Mexico tidal saline wetlands along macroclimatic gradients. a, Heat maps and contour lines illustrate the distributions of the four dominant coastal wetland plant functional groups. **b**, Integration of all four groups (group colours are consistent with the exception of succulents, which are denoted by black stippling).

and availability will better equip coastal wetland scientists with the tools needed to develop comprehensive ecological models that simultaneously evaluate the effects of SLR, macroclimate, and other climate and land-use change factors.

Many coastal wetland ecosystems around the world are vulnerable to climate-driven changes in foundation plant species type and/or abundance, which has major implications for future provisioning of their extraordinarily valuable ecosystem services and their suitability as habitat for fish and wildlife species[5,13]. Building on our targeted study design and sampling across regional climatic gradients, our relatively simple macroclimatic models are the first we know of to quantify the influence of rainfall and temperature

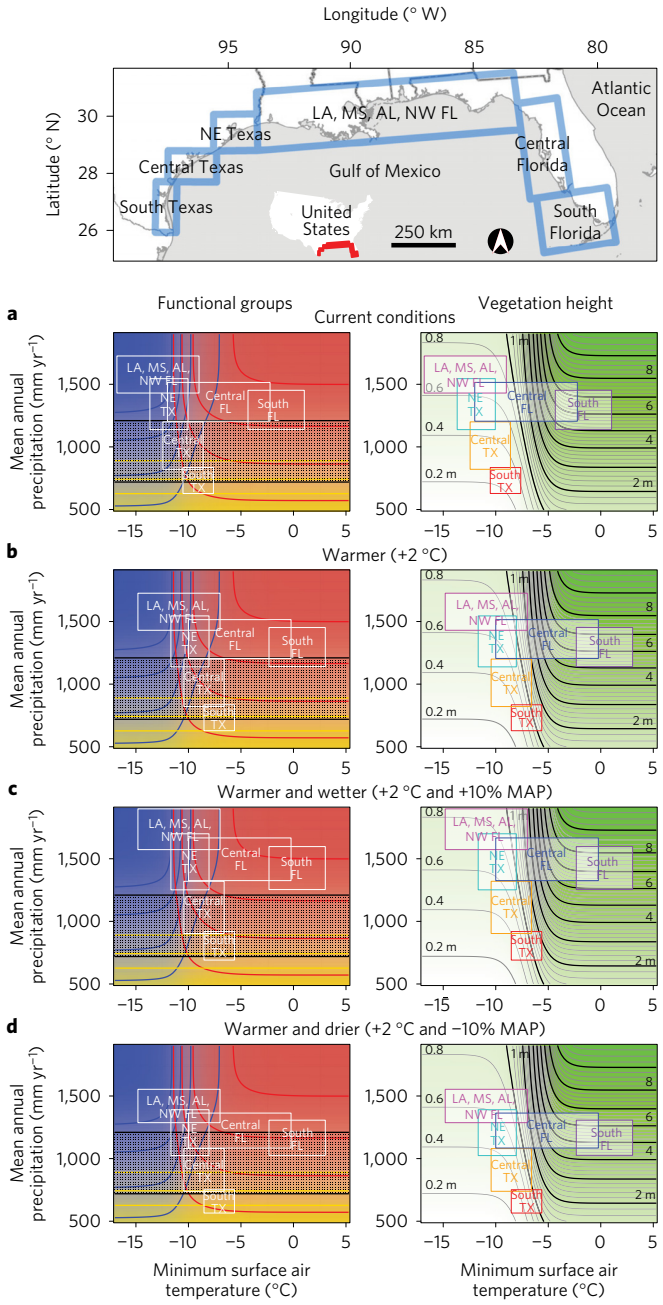

Figure 5 | Distributions of plant functional groups and vegetation height along macroclimatic gradients, with representations of current climatic and alternative low-emission future climatic conditions for select coastal reaches in the northern Gulf of Mexico. The map shows the boundaries of six northern Gulf of Mexico coastal reaches (Methods). **a**–**d**, Heat maps and contour lines illustrate group dominance (left) and vegetation height (right). Functional groups include: blue, graminoids; red, mangroves; black stippling, succulents; yellow, unvegetated. Coloured contours (left) denote 20% dominance intervals. Rectangles in **a**–**d** illustrate ranges of climatic conditions within the six coastal reaches depicted in the map under the climate conditions described for each pair of panels. LA, Louisiana; MS, Mississippi; AL, Alabama; NW FL, northwest Florida; NE TX, northeast Texas.

upon the dominant coastal wetland plant functional groups, and the first to model these plant communities across temperature and precipitation gradients simultaneously at a landscape scale. These models illustrate climate–vegetation linkages, substantiate existing macroclimatic hypotheses, and predict considerable changes in plant community structure under projected climate change. The NGOM coast possesses broad climatic gradients and a suite of foundation plant functional groups representative of many coastal regions around the world[5]. Therefore, we believe that these models can inform conservation and restoration efforts beyond our focal region, and that this approach can be adapted using local data to reliably model plant community structure in the many coastal regions around the world that possess the same functional groups and are subject to similar macroclimatic regulation.

Methods

Methods, including statements of data availability and any associated accession codes and references, are available in the online version of this paper.

Received 25 December 2015; accepted 15 December 2016; published online 23 January 2017

References

1. Gedan, K. B., Silliman, B. R. & Bertness, M. D. Centuries of human-driven change in salt marsh ecosystems. *Annu. Rev. Mar. Sci.* **1,** 117–141 (2009).
2. McKee, K., Rogers, K. & Saintilan, N. in *Global Change and the Function and Distribution of Wetlands: Global Change Ecology and Wetlands* (ed. Middleton, B. A.) 63–96 (Springer, 2012).
3. Morris, J. T., Sundareshwar, P. V., Nietch, C. T., Kjerfve, B. & Cahoon, D. R. Responses of coastal wetlands to rising sea level. *Ecology* **83,** 2869–2877 (2002).
4. Whittaker, R. H. *Communities and Ecosystems* (Macmillan, 1975).
5. Osland, M. J. *et al*. Beyond just sea-level rise: considering macroclimatic drivers within coastal wetland vulnerability assessments to climate change. *Glob. Change Biol.* **22,** 1–11 (2016).
6. Osland, M. J., Enwright, N., Day, R. H. & Doyle, T. W. Winter climate change and coastal wetland foundation species: salt marshes vs. mangrove forests in the southeastern United States. *Glob. Change Biol.* **19,** 1482–1494 (2013).
7. Cavanaugh, K. C. *et al*. Poleward expansion of mangroves is a threshold response to decreased frequency of extreme cold events. *Proc. Natl Acad. Sci. USA* **111,** 723–727 (2014).
8. Cavanaugh, K. C. *et al*. Integrating physiological threshold experiments with climate modeling to project mangrove species' range expansion. *Glob. Change Biol.* **21,** 1928–1938 (2015).
9. Saintilan, N., Wilson, N. C., Rogers, K., Rajkaran, A. & Krauss, K. W. Mangrove expansion and salt marsh decline at mangrove poleward limits. *Glob. Change Biol.* **20,** 147–157 (2014).
10. Alongi, D. M. The impact of climate change on mangrove forests. *Curr. Clim. Change Rep.* **1,** 30–39 (2015).
11. Montagna, P., Gibeaut, J. & Tunnell, J. W. J. in *The Changing Climate of South Texas 1900–2100: Problems and Prospects, Impacts and Implications—CREST-RESSACA* (eds Norwine, J. & Kuruvilla, J.) 57–77 (Texas A&M Univ., 2007).
12. Osland, M. J., Enwright, N. & Stagg, C. L. Freshwater availability and coastal wetland foundation species: ecological transitions along a rainfall gradient. *Ecology* **95,** 2789–2802 (2014).
13. Ellison, A. M. *et al*. Loss of foundation species: consequences for the structure and dynamics of forested ecosystems. *Front. Ecol. Environ.* **3,** 479–486 (2005).
14. Bianchi, T. S. *et al*. Historical reconstruction of mangrove expansion in the Gulf of Mexico: linking climate change with carbon sequestration in coastal wetlands. *Estuar. Coast. Shelf Sci.* **119,** 7–16 (2013).
15. Doughty, C. L. *et al*. Mangrove range expansion rapidly increases coastal wetland carbon storage. *Estuar. Coast.* **39,** 385–396 (2016).
16. Yando, E. S. *et al*. Salt marsh-mangrove ecotones: using structural gradients to investigate the effects of woody plant encroachment on plant-soil interactions and ecosystem carbon pools. *J. Ecol.* **104,** 1020–1031 (2016).
17. Millennium Ecosystem Assessment *Ecosystems and Human Well-Being—Synthesis Report* (World Resources Institute, 2005).
18. Barbier, E. B. *et al*. The value of estuarine and coastal ecosystem services. *Ecol. Monogr.* **81,** 169–193 (2011).
19. De Groot, R. *et al*. Global estimates of the value of ecosystems and their services in monetary units. *Ecosys. Serv.* **1,** 50–61 (2012).
20. Glick, P., Stein, B. & Edelson, N. *Scanning the Conservation Horizon: A Guide to Climate Change Vulnerability Assessment* (National Wildlife Federation, 2011).
21. Twilley, R. R. & Day, J. W. in *Estuarine Ecology* (eds Day, J. W., Crump, B. C., Kemp, M. W. & Yanez-Arancibia, A.) 165–202 (Wiley, 2012).
22. Pennings, S. C., Siska, E. L. & Bertness, M. D. Latitudinal differences in plant palatability in Atlantic coast salt marshes. *Ecology* **82,** 1344–1359 (2001).
23. Zedler, J. *The Ecology of Southern California Coastal Salt Marshes: A Community Profile FWS/OBS-81/54* (US Fish and Wildlife Service, 1982).

24. Guo, H. Y., Zhang, Y. H., Lan, Z. J. & Pennings, S. C. Biotic interactions mediate the expansion of black mangrove (*Avicennia germinans*) into salt marshes under climate change. *Glob. Change Biol.* **19,** 2765–2774 (2013).
25. Armitage, A. R., Highfield, W. E., Brody, S. D. & Louchouarn, P. The contribution of mangrove expansion to salt marsh loss on the Texas Gulf Coast. *PLoS ONE* **10,** e0125404 (2015).
26. Osland, M. J. *et al*. Mangrove expansion and contraction at a poleward range limit: climate extremes and land-ocean temperature gradients. *Ecology* **98,** 125–137 (2017).
27. Eslami-Andargoli, L., Dale, P., Sipe, N. & Chaseling, J. Mangrove expansion and rainfall patterns in Moreton Bay, southeast Queensland, Australia. *Estuar. Coast. Shelf Sci.* **85,** 292–298 (2009).
28. Kirwan, M. L. & Megonigal, J. P. Tidal wetland stability in the face of human impacts and sea-level rise. *Nature* **504,** 53–60 (2013).
29. Krauss, K. W. *et al*. How mangrove forests adjust to rising sea level. *New Phytol.* **202,** 19–34 (2014).
30. Kirwan, M. L., Temmerman, S., Skeehan, E. E., Guntenspergen, G. R. & Fagherazzi, S. Overestimation of marsh vulnerability to sea level rise. *Nat. Clim. Change* **6,** 253–260 (2016).

Acknowledgements

We are grateful for the support of the US Department of the Interior South Central Climate Science Center, US Geological Survey's Ecosystems Mission Area, US Geological Survey's Climate and Land Use Change R&D Program, Gulf Coastal Plains and Ozarks Landscape Conservation Cooperative, and the University of Houston. For facilitating our field collections, we thank Padre Island National Seashore, Texas Parks and Wildlife Department, King Ranch, Coastal Bend Bays and Estuaries Program, Hillsborough County, Manatee County, multiple US Fish and Wildlife Service National Wildlife Refuges, and multiple National Estuarine Research Reserves. C.A.G. thanks J. Gabler for numerical modelling assistance. We thank K. Krauss for a thoughtful manuscript review. Any use of trade, firm, or product names is for descriptive purposes only and does not imply endorsement by the US Government.

Author contributions

All authors helped design the project and data collection protocols. C.A.G., M.J.O., A.S.F., M.L.M., J.L.M., N.M.E., R.H.D. and S.B.H. collected the data. C.A.G. analysed the data and created the figures. C.A.G. and M.J.O. wrote the first manuscript draft, and all authors contributed to revisions.

Additional information

Supplementary information is available in the online version of the paper. Reprints and permissions information is available online at www.nature.com/reprints. Correspondence and requests for materials should be addressed to C.A.G.

Competing financial interests

The authors declare no competing financial interests.

Methods

Study areas and sampling design. We collected field data within ten estuaries that spanned the northern Gulf of Mexico (NGOM) coast. Estuaries were selected based upon their position along the ecologically relevant precipitation and winter temperature gradients present within the region[5,6,11,12]. Supplementary Table 1 summarizes the location, climate, and physical properties of each focal estuary.

Within each estuary, we sampled along 6–8 transects (70 transects in total). We positioned transects so as to capture estuary-scale salinity and elevation gradients, as well as the representative vegetation zones observed within the tidal saline wetlands of a given estuary. All transects were oriented roughly perpendicularly to the shoreline.

For each transect, we employed a sampling protocol designed to capture the entire tidal saline wetland elevation gradient, as well as all the transitions between vegetative zones within tidal saline wetlands. We began each transect in open water and positioned 1-m^2 plots where we encountered at least one of the following three criteria: a vegetation transition criterion (that is, a clear transition zone or ecotone between two visibly different plant communities); an elevation criterion (that is, a 15-cm increase or decrease in elevation relative to the previous plot); or a distance criterion (that is, a horizontal movement of 20 m from the previous plot with neither a change in vegetation zone nor a 15-cm change in elevation). Where we met the elevation or distance criterion but not the vegetation criterion, we placed only one plot. Where we encountered a vegetation transition zone, we placed a total of three plots (that is, one plot on the shoreward side of the transition, one plot at the centre of the transition, and one plot on the landward side of the transition). The vegetation in plots located shoreward or landward of a transition zone was characteristic of its respective side of the ecotone, while the vegetation in the central plots contained an approximately equal mixture of plant communities from both sides of the transition zone. For abrupt transition zones, the central plots often had two halves dominated by different species. For diffuse transition zones, the central plots often contained a scattered mixture of the species present on either side of the transition zone. Where multiple vegetation transition zones were present within a small area (for example, an area the size of one or two 1-m^2 plots), we placed multiple 1-m^2 plots side by side across the multiple transition zones. Finally, when we encountered conspicuous shifts in vegetation height or density, or in the composition of non-dominant species, we included additional 1-m^2 plots to characterize these changes.

We ended a transect when: either the plot elevation exceeded two tidal ranges (that is, two Great Diurnal Ranges) above mean lower low water; or when we moved two 20-m distance increments without encountering a vegetation transition zone or a 15-cm change in elevation (that is, the distance criterion was used consecutively). Note that the goal of this design was not to accurately quantify and compare estuary-scale vegetation coverage, but rather to quantify abiotic–biotic linkages across relatively dramatic local and regional abiotic gradients. Within each estuary, we sampled a total of between 87 and 122 1-m^2 plots. For the entire study (that is, across all ten estuaries), we sampled a total of 1,020 1-m^2 plots.

Plant data. Within each 1-m^2 plot, we estimated the percentage of plant cover above and below 1.4 m separately for all species. We measured mean and maximum vegetation canopy heights, and recorded the species of the tallest individual present within each plot. We quantified light [that is, photosynthetically active radiation (PAR)] interception in each plot using a linear ceptometer (AccuPAR LP-80, Decagon Devices). For short-statured vegetation, we measured light intensity at ground level and above the vegetation canopy. For tall-statured vegetation (for example, forests), we measured light at ground level within the plot and at a height of 1.4 m outside the canopy in unobstructed sunlight. We calculated a proxy for standing aboveground plant biomass by multiplying the mean canopy height by the proportion of PAR intercepted. We used this simple biomass proxy to further quantify the variation in physical structure of vegetation across abiotic gradients.

Elevation data. The elevation (NAVD88) and horizontal position of each 1-m^2 plot were determined using a high-precision Global Navigation Satellite System (GNSS) (Trimble R8 and TSC3, Trimble), in combination with real-time Continuously Operating Reference Station (CORS) networks where available (that is, the Louisiana State University GULFNet network, the Texas Department of Transportation network). We transformed plot-specific elevation measurements to elevations relative to a locally relevant tidal datum [specifically, mean higher high water (MHHW)] via the use of the National Oceanic and Atmospheric Administration's (NOAA) VDatum software tool version 3.1 (ref. 31).

Climate data. We obtained climate data for the 30-year period from 1981–2010. For precipitation and temperature, we obtained continuous gridded climate data created using the Parameter-elevation Relationship on Independent Slopes Model (PRISM) interpolation method[32] by the PRISM Climate Group (Oregon State University; http://prism.oregonstate.edu). We used Esri ArcMap 10.2.2 (Redlands, California, USA) to extract the 30-year mean annual precipitation (MAP) and the 30-year absolute minimum temperature (minT) (that is, the lowest temperature recorded during the 30-year period) from the gridded PRISM data for each of our study plots[33]. The spatial resolution of the MAP gridded data was 800 m and the spatial resolution of the minT gridded data was 4 km. These variables were selected based upon the results of Osland and colleagues[6,12].

Data analyses: elevation boundaries. Since the focus of our study was on tidal saline wetlands, we needed to identify the estuary-specific upper and lower boundaries of the tidal saline wetland zone to restrict our analyses solely to those plots located within this zone. From the literature, we identified qualitative vegetation-based zonation transitions that characterize the upper and lower boundaries of the tidal saline wetland zone within each estuary (Supplementary Table 2). We used these boundaries to assign a binary code to each plot designating whether the plot was within or outside of the tidal saline wetland zone. Via this process, 602 plots were designated as being within the tidal saline wetland zone, whereas 418 plots were designated as being outside of this zone.

Next, we used logistic regression to quantify the vertical position of these boundaries relative to a tidal datum (MHHW). For each estuary, we used two logistic regressions (that is, one regression each for the upper and lower boundaries) to quantify the relationship between elevation relative to MHHW (independent variable) and tidal saline wetland presence/absence (response variable). We used these equations to quantify three summary elevations for each upper and lower boundary for each estuary-specific tidal saline wetland zone (Supplementary Table 3). Each set of three summary elevations includes calculations of the local maximum of the first derivative (that is, the threshold), and the local minimum and maximum peaks of the second derivative of the associated logistic regression (that is, the upper and lower inflection points)[12,34,35].

We quantified normalized elevation quartiles for each estuary by defining the minimum and maximum elevations as the elevations relative to MHHW of the lowest (E_{min}) and highest (E_{max}) plots that we designated as being within the tidal saline wetland zone; we then divided this elevation range into four equal segments. Since each estuary's tidal saline wetlands spanned a different elevation range, we normalized plot elevations within estuaries by calculating the relative elevation (E_{rel}) of each plot using the following equation: $E_{rel} = (E_{plot} - E_{min})/(E_{max} - E_{min})$, where E_{plot} is the elevation of a plot relative to MHHW. This calculation produced normalized elevation values for plots that ranged from 0 to 1, and all tidal saline wetlands plots within each estuary were assigned to an elevation quartile (with quartile boundaries of 0.25, 0.5, and 0.75) based on their relative elevation (E_{rel}). To minimize variation among estuaries arising from differences in the abundance of plots within elevation quartiles, elevation quartiles were weighted equally regardless of the number of plots in each.

Data analyses: plant functional groups. Each plant species observed within the tidal saline wetland zone was assigned to one of six functional groups: graminoids, mangroves, succulents, vines, non-succulent forbs, or ferns. The graminoid group included grasses, sedges, and rushes (that is, species in the Poaceae, Cyperaceae, and Juncaceae families, respectively). The mangrove group included woody trees and shrubs adapted to tidal saline wetland environments[36]. The succulent group included halophytic forbs and shrubs with fleshy, water-storing leaves and/or stems. Succulent plants regulate their internal salt concentrations via osmotic adjustment of cell storage volumes[37,38]. We excluded the vine, non-succulent forb, and fern groups from further analysis because their combined average ground cover was very low (less than 0.3%) and they were found in only 4.2% of the plots. Graminoids, mangroves, and succulents dominated the tidal saline wetland zone across all estuaries and were the primary focus of this study (Fig. 1). We also defined and considered an 'unvegetated' functional group, which included barren areas as well as areas containing photosynthetic microbial mats comprised of filamentous algae, cyanobacteria and other microbiota. Supplementary Table 4 lists all of the 39 species observed within the tidal saline wetland zone and their assigned functional group.

Plant functional group dominance was summarized for each estuary by calculating the mean proportion of plots dominated by each functional group class across all four normalized elevation quartiles (Fig. 2). The following four functional group classes were evaluated: graminoids, mangroves, succulents, and unvegetated. Plots with less than 25% total plant cover were considered unvegetated. When total plant cover was at least 25%, dominance within a plot was defined as the functional group (that is, graminoids, mangroves, or succulents) with the greatest cover. For example, if mangroves dominated 100% of tidal saline wetland plots in elevation quartile 1 within a given estuary, 20% of plots in elevation quartile 2, and 0% in quartiles 3 and 4, the mangrove dominance value for that estuary would be 30% ((100% + 20% + 0% + 0%)/4). Average vegetation height and biomass proxy values were calculated similarly for each estuary using equally weighted averages from each elevation quartile. Summarizing plant community structure in this manner is a significant simplification, but it is both appropriate, given the variability in coastal wetlands at fine spatial and temporal scales, and necessary to model landscape-scale patterns.

Data analyses: climate–vegetation linkages. One of our primary objectives was to use our field-based and functional group-specific data to test and expand upon previous climate–vegetation linkages developed for the NGOM. The distribution of mangrove forests relative to graminoid-dominated salt marshes has been shown to be controlled by the frequency and intensity of winter extreme low air temperature events[6]. Total plant coverage in tidal saline wetlands has been shown to be controlled by rainfall and freshwater availability[12]. These studies identified minT and MAP, respectively, as climatic variables that greatly influence the structure and function of tidal saline wetlands in the region. However, neither of these studies quantified the effects of the interaction between minT and MAP. Moreover, both of these studies used image-based tidal saline wetland data that neither explicitly characterized species composition or vegetation structure, nor distinguished between four dominant functional groups, as we have done here.

We used our data to evaluate the independent and interactive effects of MAP and minT upon plant functional group dominance, vegetation height, and the aboveground biomass proxy. First, we used nonlinear least squares (NLS) regression to quantify the independent relationships between each of the two climate variables (that is, MAP and minT) and the response variables (that is, dominance of each of the four functional groups, vegetation height, and the aboveground biomass proxy) (Fig. 3). Sigmoidal functions provided the best model fit for all relationships between climate and vegetation variables, except for the relationship between MAP and succulent dominance, which was best modelled with a Gaussian (normal) function. We excluded the two Florida estuaries when fitting the relationship between MAP and vegetation height (Fig. 3d) because they are outliers in this context. Mangroves are much taller than graminoids or succulents, so it is inappropriate to model height using estuaries overwhelmingly dominated by these different groups at the same time. However, we expect that the relationship between MAP and vegetation height in mangrove-dominated communities is proportionally similar to their relationship in graminoid- and succulent-dominated communities[39,40]. That is, we observed a sixfold increase in vegetation height (from about 20 to 120 cm) along the MAP gradient among the eight estuaries in Fig. 3d, and we would likewise expect a sixfold increase in height (perhaps, for example, from 2 to 12 m) along the same MAP gradient among mangrove-dominated estuaries. There is a physiological basis for this; as drought and/or salinity stress increases, mangrove vessel architecture narrows, which limits plant height[39–42]. Total mangrove cover would also decrease as drought and/or salinity stress increases[11,12], and these height values represent estuary-wide averages. Had we sampled additional mangrove-dominated estuaries at more points along a MAP gradient, we believe we could have produced a similar curve by modelling those estuaries. Therefore, we modelled the relationship between MAP and height in the eight estuaries shown in Fig. 3d using a unitless, proportional metric (mean vegetation height/maximum mean vegetation height), which allowed us to use the equation for its best-fit curve to model height in mangrove-dominated estuaries as well.

Next, we used these equations to develop heat maps and contour plots that illustrate functional group distributions and vegetation height along both temperature (minT) and precipitation (MAP) gradients. To generate these three-dimensional plots, we used the equations produced by our NLS regressions in the combinations specified in Supplementary Table 5 to populate matrices of projected response variable values across continuous ranges of minT and MAP. Raw projections from these equations are presented for individual functional groups (Fig. 4a) and vegetation height (Fig. 5, right; Supplementary Fig. 1, right). In figures that integrate all four functional groups (Fig. 4b and Fig. 5, left; Supplementary Fig. 1, left), we arithmetically adjusted each group's projected dominance value for each matrix cell so that the relative proportions of groups remained the same but the sum of all groups equalled one. Height and biomass proxy projections required normalization and use of a global maximum scaling factor (see Supplementary Table 5), so we used the maxima among transects as scaling factors for both. Collectively, these analyses and mathematical models enabled us to quantify and illustrate the variation in functional group dominance and vegetation structure within macroclimatic space.

Data analyses: current and future climate. For illustrative purposes, we depict the locations of six different coastal reaches within bivariate macroclimatic space under current and potential future climatic conditions. We accomplished this by first calculating the current climate conditions within tidal saline wetland zones in the following six coastal reaches of the NGOM: south Texas (25.96° to 27.74° latitude, −97.84° to −97.03° longitude); central Texas (27.74° to 28.81°, −97.39° to −95.48°); northeast Texas (28.81° to 30.08°, −95.59° to −93.85°); Louisiana, Mississippi, Alabama, and northwest Florida (28.81° to 30.83°, −93.85° to −83.43°); central Florida (26.39° to 29.74°, −83.43° to −81.83°); and south Florida (24.45° to 26.39°, −83.18° to −80.44°). These six reaches were selected because they each represent distinct climate-controlled tidal saline wetland ecological zones. For each of these coastal reaches, we used the PRISM gridded climate data described previously and the US Fish and Wildlife Service National Wetlands Inventory[43] to obtain the range of climatic conditions (that is, MAP and minT) present within tidal saline wetland zones of each reach. These climatic ranges are depicted as rectangles denoting the minimum and maximum MAP and minT within each coastal reach (Fig. 5a and Supplementary Figs 1a and 2a).

Potential future climates are similarly presented as rectangles denoting upper and lower extremes for MAP and minT within coastal reaches. All potential future climate scenarios we present are simple arithmetic adjustments to current climate values derived from 1981–2010 observations (Fig. 5b–d and Supplementary Figs 1b–d and 2b–g). That is, our potential future climate rectangles are simply current temperatures +2 °C or +4 °C for minT, and/or current MAP multiplied by 1.1 or 0.9 for a 10% increase or 10% decrease in precipitation, respectively. Although these are not actual climate predictions, the +2 °C and +4 °C scenarios are within the range of future conditions predicted by Coupled Model Intercomparison Project Phase 5 (CMIP5) models under greenhouse gas concentration scenarios Representative Concentration Pathway (RCP) 4.5 and RCP8.5, respectively[44]. Importantly, particular projections are similar to downscaled CMIP5 ensemble predictions for specific portions of the NGOM coast (Multivariate Adaptive Constructed Analogs (MACA) data set[45,46]). Specifically, the +2 °C and −10% MAP projection is similar to scenario RCP4.5 for Texas and Louisiana; the +2 °C and +10% MAP projection is similar to RCP4.5 for Mississippi, Alabama, and Florida; and the +4 °C and −10% MAP projection is similar to RCP8.5 for Texas, Louisiana, Mississippi, Alabama, and over 90% of Florida. Note that ensemble MAP projections for these scenarios are actually intervals (±0–10%), so a change of ±10% represents the extreme limits of the ensemble projections; however, some individual model projections for MAP exceed ±10% in these coastal reaches. There is strong agreement among downscaled CMIP5 models[45,46] (even under conservative scenarios) that minimum temperatures will increase ∼2 °C or more by 2100 across the NGOM coast. Increases of ∼4 °C are likely only under the highest concentration scenario (RCP8.5). There is considerable variability among CMIP5 models regarding projected changes in rainfall. Differences between MAP projections from individual models under the moderate RCP4.5 scenario are large for Texas, Louisiana, and south Florida, with some models predicting increases in MAP and others decreases. Models largely agree that precipitation will decrease to some extent under RCP8.5.

Data availability. Source data are available at https://www.sciencebase.gov/catalog/item/57b24094e4b00148d3982cce.

References

31. VDatum Version 3.4 (NOAA, 2015); http://vdatum.noaa.gov
32. Daly, C. *et al*. Physiographically sensitive mapping of climatological temperature and precipitation across the conterminous United States. *Int. J. Climatol.* **28,** 2031–2064 (2008).
33. PRISM Climate Group, Oregon State Univ. (2015); http://prism.oregonstate.edu
34. Frazier, A. E. & Wang, L. Modeling landscape structure response across a gradient of land cover intensity. *Landsc. Ecol.* **28,** 233–246 (2013).
35. Hufkens, K., Ceulemans, R. & Scheunders, P. Estimating the ecotone width in patchy ecotones using a sigmoid wave approach. *Ecol. Inform.* **3,** 97–104 (2008).
36. Tomlinson, P. B. *The Botany of Mangroves* (Cambridge Univ. Press, 1986).
37. Flowers, T. J., Troke, P. F. & Yeo, A. R. The mechanism of salt tolerance in halophytes. *Annu. Rev. Plant Physiol.* **28,** 89–121 (1977).
38. Khan, M. A., Ungar, I. A. & Showalter, A. M. The effect of salinity on the growth, water status, and ion content of a leaf succulent perennial halophyte, *Suaeda fruticosa* (L.) Forssk. *J. Arid. Environ.* **45,** 73–84 (2000).
39. Lot-Helgueras, A., Vázquez-Yanes, C. & Menendez, F. in *Proceedings of the International Symposium on Biology and Management of Mangroves* (eds Walsh, G. E., Snedaker, S. C. & Teas, H. J.) 52–64 (Institute of Food and Agricultural Sciences, Univ. Florida, 1975).
40. Méndez-Alonzo, R., López-Portillo, J. & Rivera-Monroy, V. H. Latitudinal variation in leaf and tree traits of the mangrove *Avicennia germinans* (Avicenniaceae) in the central region of the Gulf of Mexico. *Biotropica* **40,** 449–456 (2008).
41. Lugo, A. E. & Patterson-Zucca, C. The impact of low temperature stress on mangrove structure and growth. *Trop. Ecol.* **18,** 149–161 (1977).
42. Madrid, E. N., Armitage, A. R. & López-Portillo, J. *Avicennia germinans* (black mangrove) vessel architecture is linked to chilling and salinity tolerance in the Gulf of Mexico. *Front. Plant Sci.* **5,** 00503 (2014).
43. *National Wetlands Inventory* (US Fish and Wildlife Service, 2015); http://www.fws.gov/wetlands
44. IPCC *Climate Change 2013: The Physical Science Basis* (Cambridge Univ. Press, 2013).
45. Abatzoglou, J. T. Development of gridded surface meteorological data for ecological applications and modelling. *Int. J. Climatol.* **33,** 121–131 (2013).
46. Livneh, B. *et al*. A long-term hydrologically based dataset of land surface fluxes and states for the conterminous United States: update and extensions. *J. Clim.* **26,** 9384–9392 (2013).